



Separable structural requirements for cDNA synthesis, nontemplated extension, and template jumping by a non-LTR retroelement reverse transcriptase

Received for publication, November 29, 2021, and in revised form, January 12, 2022. Published, Papers in Press, January 21, 2022.

<https://doi.org/10.1016/j.jbc.2022.101624>

Sydney C. Pimentel¹, Heather E. Upton, and Kathleen Collins*

From the Department of Molecular and Cell Biology, University of California at Berkeley, Berkeley, California, USA

Edited by Karin Musier-Forsyth

Broad evolutionary expansion of polymerase families has enabled specialization of their activities for distinct cellular roles. In addition to template-complementary synthesis, many polymerases extend their duplex products by nontemplated nucleotide addition (NTA). This activity is exploited for laboratory strategies of cloning and sequencing nucleic acids and could have important biological function, although the latter has been challenging to test without separation-of-function mutations. Several retroelement and retroviral reverse transcriptases (RTs) support NTA and also template jumping, by which the RT performs continuous complementary DNA (cDNA) synthesis using physically separate templates. Previous studies that aimed to dissect the relationship between NTA and template jumping leave open questions about structural requirements for each activity and their interdependence. Here, we characterize the structural requirements for cDNA synthesis, NTA, template jumping, and the unique terminal transferase activity of *Bombyx mori* R2 non-long terminal repeat retroelement RT. With sequence alignments and structure modeling to guide mutagenesis, we generated enzyme variants across motifs generally conserved or specific to RT subgroups. Enzyme variants had diverse NTA profiles not correlated with other changes in cDNA synthesis activity or template jumping. Using these enzyme variants and panels of activity assay conditions, we show that template jumping requires NTA. However, template jumping by NTA-deficient enzymes can be rescued using primer duplex with a specific length of 3' overhang. Our findings clarify the relationship between NTA and template jumping as well as additional activities of non-long terminal repeat RTs, with implications for the specialization of RT biological functions and laboratory applications.

Reverse transcriptases (RTs) are an evolutionarily diverse group of enzymes defined by their ability to synthesize DNA from an RNA template. Reverse transcriptase activity is fundamental to the perpetuation of selfish retroelements in all domains of life (1). In addition, RTs function in bacterial host defense, generate sequence diversity in phage and bacterial

genes, and maintain eukaryotic chromosome ends (1, 2). From a biotechnological perspective, their ability to synthesize complementary DNA (cDNA) from both RNA and DNA templates is routinely exploited for laboratory and clinical applications including RNA-seq and RT-PCR. However, despite remarkable RT phylogenetic diversity, most applications rely exclusively on the recently branched retroviral RTs engineered by iterations of mutagenesis over the past several decades (3). Other retroelements include the eukaryotic long terminal repeat (LTR) retroelements, from which retroviral RTs emerged, and also the more ancestral non-LTR retroelements (4, 5). Unlike their evolutionary predecessors, retroviral RT active site features are adapted to benefit virus reproduction rather than perpetuation within the host genome. Retroviral enzymes are therefore insufficient model systems for understanding the complexity of selfish retroelement RT structures and activities. Understanding the properties of these retroelement RTs will provide a foundation for further optimization of biotechnological applications as well as insights into the RT properties necessary for retroelement propagation.

Sequence alignments and structural characterization support an overall RT active site architecture that can be envisioned as a right-handed arrangement of fingers, palm, and thumb subdomains (6, 7). Reverse transcriptases and also viral RNA-dependent RNA polymerases (RdRPs) share seven primary sequence motifs, 1 to 7 (8, 9). RNA-dependent RNA polymerases and non-viral RTs also share subsets of additional insertion motifs (Fig. 1A), typically termed 2a, 3a, 4a, 6a, and 7a, as well as an N-terminal extension that can include motifs 0 and -1 (10–12). Structure determination and mutagenesis studies of a limited number of bacterial mobile group II intron RTs and eukaryotic telomerase RTs indicate that motif insertions are tailored by evolution to adapt RTs to their biological functions (13–17).

Compared to retroviral, intron, and telomerase RTs, relatively little is known about eukaryotic non-LTR retroelement RT structure-function relationships. Non-LTR retroelement subgroups are distinguished by the number of ORFs and the presence of additional domains in the ORF encoding the RT (4, 18). A widespread early-branching group has a single ORF, with the central RT domain followed by a C-terminal

* For correspondence: Kathleen Collins, kcollins@berkeley.edu.

We sought to determine the structural features of a eukaryotic non-LTR retroelement RT that allow it to perform NTA and template jumping and to investigate the interrelation of these two activities. We designed a library of over 100 sequence variants of *B. mori* R2 RT with side-chain substitutions across the N-terminal extension, fingers, palm, and thumb subdomains. Mutations were guided by multiple sequence alignment and protein structure prediction. Overall, our results provide the most detailed analysis to date of the structural requirements for the activities of a non-LTR retroelement RT. Among our conclusions, we demonstrate that NTA is a prerequisite for template jumping but can be bypassed using a primer duplex with the optimal length of 3' overhang. Our findings provide insight into the requirements for cDNA synthesis initiation by the TPRT mechanism of non-LTR retroelement mobility and will enable expansion of RT applications to research and medicine.

Results

Design and cDNA synthesis activity of RT sequence variants

As a model non-LTR retroelement RT, we used a highly active, extensively purified version of *B. mori* R2 protein, designated BoMoC, which lacks the N-terminal sequence-specific DNA-binding domains (Fig. 1A, bottom) (29). To guide structure/function analysis, we used multiple sequence alignments to define the boundaries of shared RT motifs in BoMoC. The resulting sequence annotations largely agree with those reported by the Eickbush and Christensen labs (10, 12), with minor adjustments (Fig. S1). In addition, we generated a protein structure prediction for the R2 RT domain using Phyre2 (Fig. 1B). Both the caliciviral rabbit hemorrhagic RdRP (PDB 1KHV) and a thermostable group II intron RT (PDB 6AR3) were used as templates to create the R2 RT structure prediction (7, 15). Additional comparisons used the structure of the spliceosome protein Prp8 (39), which contains an inactivated RT domain speculated to be present due to evolution of the spliceosome from a mobile element ribonucleoprotein.

Mutagenesis prioritization used alignments and structure modeling to predict residues important for the specificity and efficiency of dNTP incorporation by templated and non-templated addition as well as residues potentially involved in binding primer and template nucleic acids. Ultimately, we selected side chains in motifs 0, 1, 2, 2a, 3, 7, and the thumb domain for substitution. Below, we describe the sequence-variant RTs with informative changes in product synthesis profile. BoMoC amino acid substitutions are numbered with respect to the ORF initially reported by the Eickbush lab (20), for comparison to full-length R2 RT. All side chain substitutions were to alanine or glycine. Enzyme variants were purified with Nickel-NTA resin followed by size-exclusion chromatography. Protein purity was confirmed by denaturing sodium dodecyl sulfate - polyacrylamide gel electrophoresis and direct protein staining (Fig. 1C).

BoMoC variants were first screened for the ability to synthesize cDNA on an annealed primer-template substrate, using

a DNA primer that is 10 nt shorter than the RNA template (Fig. 2A; oligonucleotide sequences are listed in Table 1). Enzymes that were inactive or indistinguishable from the WT BoMoC in their product profile were dropped from subsequent assays. Most substitutions maintained or reduced enzyme activity, but substitutions in motif 0, motif 2a, and the thumb domain increased product synthesis relative to WT BoMoC (Fig. 2B).

BoMoC variants with altered NTA

Upon completion of template copying, full-length *B. mori* R2 protein extends its cDNA product by up to three additional non-templated nt (23). Using BoMoC, NTA can be detected up to 7 nt beyond the end of the template, with strong +3 and +4 NTA products (29). BoMoC finger and palm substitutions heterogeneously decreased NTA without parallel influence on the level of cDNA synthesis activity overall (Fig. 2B). Among the BoMoC enzymes compromised for NTA, BoMoC K452A, R463A, I465A, R473A, and F534G had decreased relative activity whereas BoMoC D500A, L704A, and F708A had increased relative activity compared to WT BoMoC (Fig. 2B).

Side-chain substitutions that reduce activity have at least two roles (Fig. 3, A–C; see color-coded annotation of side-chain roles in Fig. 1C). First, motif 1 K452 and motif 2 R463 are predicted to form salt bridges to the incoming nucleotide triphosphate (Fig. 3B) as part of a dNTP-binding pocket that has structurally analogous side chains in retroviral RTs (40–42). For BoMoC, the K452A substitution results in less severe activity and NTA defects than the R463A substitution, and the K452A enzyme remains capable of template jumping to the annealed primer-template oligonucleotides present in excess (Fig. 2B, products labeled Template Jumps). Second, motif 2 I465 and R473 side chains are predicted to make template-strand contacts. The I465 side chain is predicted to stack with the templating base in the active site to promote pairing with the incoming dNTP (Fig. 3B), which could explain why BoMoC I465A has reduced NTA and reduced activity (Fig. 2B). The R473 side chain is predicted to make polar contacts to the phosphate backbone near the templating base (Fig. 3, B and C); the absence of this side chain is strongly inhibitory for BoMoC activity (Fig. 2B).

BoMoC F534G, with a side-chain substitution in motif 3 that contributes to the dNTP-binding pocket (Fig. 3B), showed some loss of activity and the most severe NTA deficiency. A large fraction of cDNA products lacked any 3' overhang (Fig. 2B, +0 products). The closest substrate feature near the F534 side chain is the deoxyribose sugar of the incoming dNTP (Fig. 3B). The analogous residue in the RT from Moloney Murine Leukemia Virus, F155, serves as a steric gate against ribonucleotides (the “sugar gate”). Moloney Murine Leukemia Virus RT substitution F155V increased binding and incorporation of NTPs (43). For comparison to BoMoC F534G and Moloney Murine Leukemia Virus RT F155V, we made an analogous amino acid substitution in the group II intron RT from *Eubacterium rectale* (14), purified with the same

Non-LTR retroelement reverse transcriptase activities

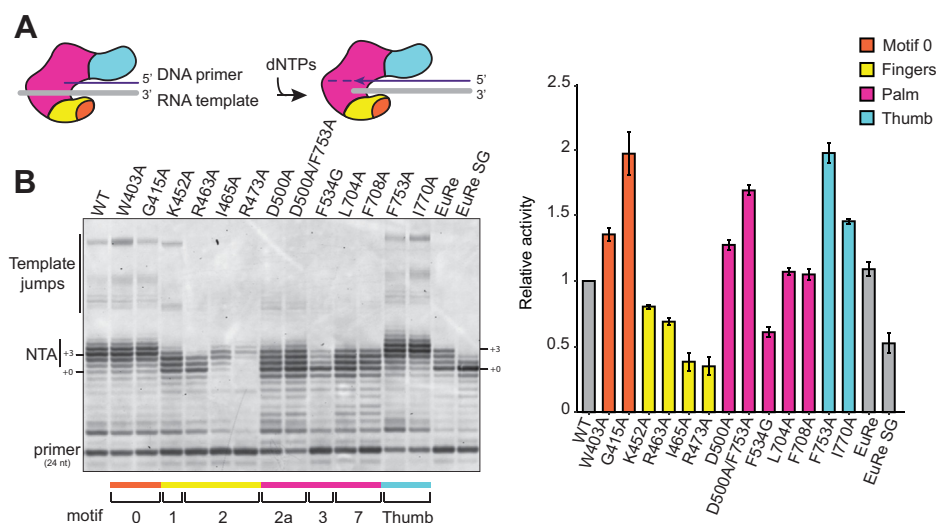


Figure 2. BoMoC variants with altered NTA activity. A, diagram of BoMoC engaged with RNA template (gray)-DNA primer (purple) duplex for fill-in cDNA synthesis. Dashed purple line indicates NTA. B, left, SYBR-gold stained denaturing urea-PAGE gel of BoMoC and EuRe cDNA extension products. Labels indicate products with +0 and +3 NTA. Right, quantification of cDNA products from fill-in synthesis, not including products labeled Template Jumps, normalized to WT. cDNA, complementary DNA; NTA, nontemplated nucleotide addition.

fusion-tag configuration as BoMoC (29). *Eubacterium rectale* intron RT (termed EuRe) has less NTA activity than BoMoC, but the EuRe sugar gate substitution F146V nonetheless decreased NTA (Fig. 2B, compare EuRe to EuRe SG). In addition, a recently published mutagenesis study demonstrated that a similar F143A substitution in a thermostable group II intron RT also decreased NTA (38), which further highlights the importance of this residue in nontemplated nt addition across a broad spectrum of RTs.

The BoMoC motif 2a substitution D500A and palm-domain substitutions L704A and F708A also compromised NTA (Fig. 2B), despite side-chain positions outside the dNTP-binding pocket (Fig. 3D). In comparison, substitution of the thumb-domain side chains of F753 or I770 (Fig. 3D) appeared to slightly increase NTA (Fig. 2B). To investigate how these side-chain substitutions influence NTA, we combined the D500A substitution and the F753A substitution to determine whether the NTA defect of D500A BoMoC could be ameliorated by the F753A-substitution activity enhancement. The double-mutant enzyme had cDNA synthesis activity

intermediate between BoMoC D500A and BoMoC F753A, but it retained the BoMoC D500A NTA defect (Fig. 2B). This finding further resolves cDNA synthesis and NTA as separable activities.

To examine the possibility that NTA defects arise from abortive template jumping, analogous to the abortive template copying responsible for “NTA” by T7 RNA polymerase (44), we assayed cDNA synthesis using a primer-template duplex with a template-strand 5' Cy3 dye (Fig. 4A; oligonucleotide sequences are listed in Table 1). This bulky modification disfavors binding of the incoming template necessary for template jumping (29) and would therefore diminish apparent NTA resulting instead from nonprocessive cDNA synthesis. BoMoC variants elongated the recessed primer 3' end to the template 5' end with relative activity levels like those observed for fill-in synthesis on the unmodified template (compare Fig. 4B to Fig. 2B). The enzymes' relative differences in NTA were also similar comparing across templates, although the product profile with the 5' Cy3 template shifted to predominantly +2 or +1 nt of NTA (Fig. 4B). BoMoC variants with R463A or

Table 1
Oligonucleotide sequences

Figure	Type	Oligonucleotide	Sequence
2	RNA	Primer extension template	AGAUCGGAAGAGCACACGUCUGAACUCCAGUCAC/3SpC3
	DNA	Primer 1 (-10 fill in)	GTGACTGGAGTTCAGACGTGTGCT
4	RNA	Primer extension Cy3 template	/5Cy3/ATTC AACCCCAAAATCTAGTGTCTG
	DNA	Primer 2 (-8 fill in)	CAGCACTAGATTTTTGG
5,6	RNA	M13 (-) RNA	UCAUAGCUGUUUCCUGUGUGA
6	DNA	Universal DNA primer	GTGACTGGAGTTCAGACGTGTGCTCTTCCGATC
	DNA	Universal DNA primer +1T	GTGACTGGAGTTCAGACGTGTGCTCTTCCGATCT
	DNA	Universal DNA primer +2TC	GTGACTGGAGTTCAGACGTGTGCTCTTCCGATCTC
	DNA	Universal DNA primer +3TCA	GTGACTGGAGTTCAGACGTGTGCTCTTCCGATCTCA
	RNA	Universal primer complement	GAUCGGAAGAmGmCmAmCmGmUmCmUmGmA mAmCmUmCmCmAmGmU/3SpC3

Ribose substitutions with 2' O-methyl ribose are indicated as “m” before the base. “3SpC3” indicates a three-carbon blocking group to prevent use of the oligonucleotide as a primer for DNA synthesis, and “5Cy3” is a 5' Cy3 dye added to inhibit use of the oligonucleotide as a jump-acceptor template. For the oligonucleotides used in Figures 2 and 4, the primer was preannealed to the primer extension template. Figure 6 primer oligonucleotides were each preannealed to the primer complement. M13 (-) RNA was used as primer in terminal transferase assays (Fig. 5) or as a jump template (Fig. 6).

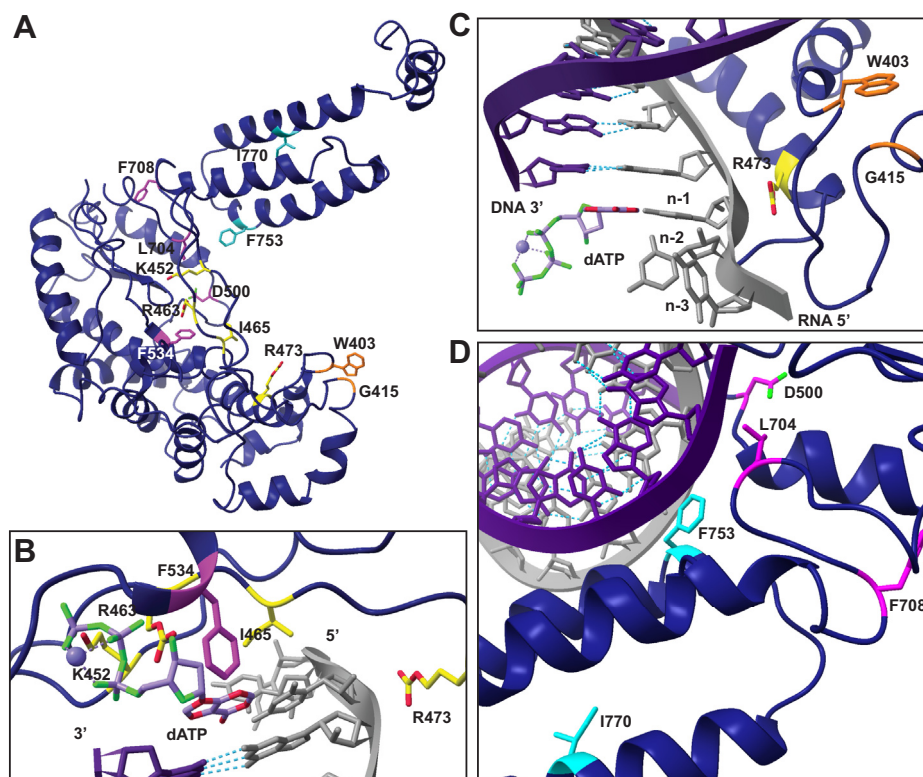


Figure 3. Side chains targeted for investigation. A, BoMoC ribbon model with colored side chains shown for the residues substituted in work described here. All side chains that were examined in this study are labeled. B and C, close-up view of dNTP-binding pocket and motif 0 residues and their proximity to unpaired RNA template and the incoming nt (dATP). RNA template (gray)-DNA primer (purple) duplex and the incoming dATP were placed using the structure of thermostable group II intron RT (PDB 6AR3). Light purple sphere indicates Mg²⁺ ion coordinated to the beta and gamma phosphates. Oxygen atoms are colored green and nitrogen atoms are colored red. Only relevant secondary structure is shown for simplicity. Unpaired template residues are labeled, with the n-1 template nt positioned to base-pair with incoming nt. D, view of motif 2a, 7, and thumb residues. RT, reverse transcriptase.

F534G substitution were the most compromised for NTA under any assay condition. In summary, all the findings described above suggest that NTA activity is particularly sensitive to changes in structural features of the dNTP-binding pocket, and that NTA has separable structural requirements from fill-in cDNA synthesis.

Separable requirements for NTA and manganese-induced terminal transferase activity

In vitro, BoMoC has a second mode of nontemplated primer elongation, which is detected in reactions containing an above-physiological concentration of manganese and therefore of uncertain biological significance. Instead of the NTA extension of the 3' end of a duplexed cDNA product, the manganese-induced terminal transferase or "tailing" activity extends single-stranded nucleic acids (29). This requires the RT to stably position single-stranded rather than duplexed primer substrate in the active site. Tailing activity differs from NTA in that tailing can add tens or hundreds of nucleotides in a processive manner and can extend ssRNA, enabling new laboratory applications of BoMoC RT (29).

To investigate BoMoC structural requirements for ssRNA tailing in relation to templated cDNA synthesis and NTA, we assayed the BoMoC variants under tailing reaction conditions (Fig. 5A; ssRNA oligonucleotide sequence is listed in Table 1).

The impact of amino acid substitutions on tailing activity was not directly correlated to impact on cDNA synthesis activity (compare Fig. 5B to Fig. 2B). Fewer of the BoMoC variants supported near-WT tailing activity than near-WT cDNA synthesis. The sharpest dichotomy was observed for the motif 7 L704A and F708A BoMoC variants: despite near-WT cDNA synthesis activity and some NTA to the cDNA duplex (Fig. 2B), these BoMoC variants had undetectable tailing activity (Fig. 5B). The motif 7 side chains L704 and F708 are in the "primer grip" motif (45) located near the DNA 3' end (Fig. 3D).

On the other hand, the BoMoC variants with increased cDNA synthesis activity showed increased ssRNA tailing activity, notable for both the motif 0 and thumb-domain substitution variants (Fig. 5B). Thumb-domain F753 extends into the duplex minor groove and contacts newly synthesized DNA whereas I770 side chain is predicted to face into a hydrophobic pocket that stabilizes three antiparallel alpha helices of the thumb domain (Fig. 3D). Thumb-domain substitutions that reduce the interaction of BoMoC with its template-product duplex could increase activity by increasing enzyme turnover, but how they could cause an increase in ssRNA tailing is less obvious. Increased ssRNA tailing was also observed for the motif 0 side chain substitutions (Fig. 5B). Compared to the thumb domain, motif 0 function is not well characterized. BoMoC side chains W403 and G415 flank a loop predicted to

Non-LTR retroelement reverse transcriptase activities

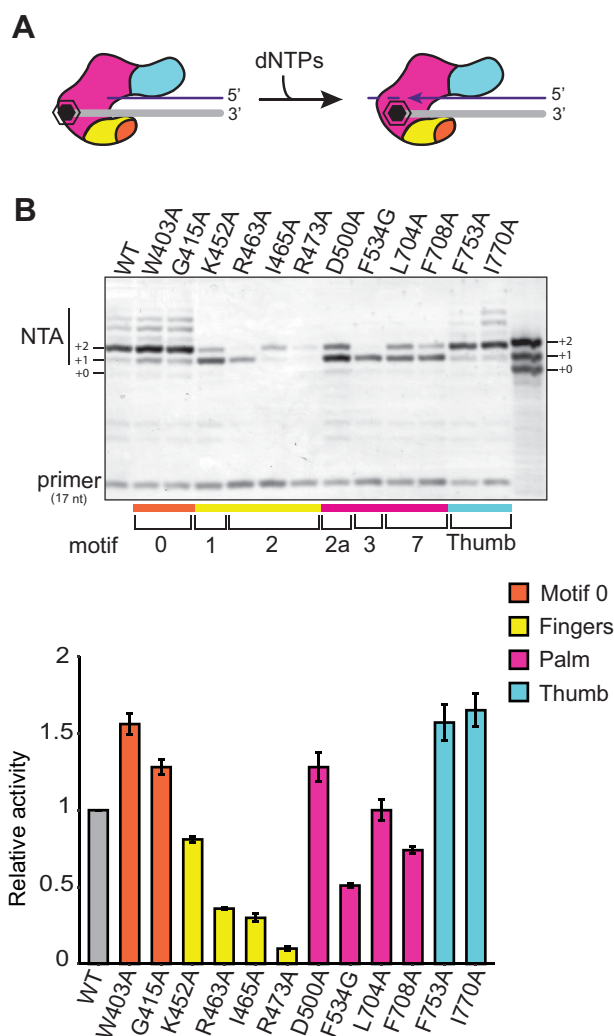


Figure 4. Independence of NTA from template jumping. A, diagram of BoMoC engaged with primer-template duplex with a template 5' Cy3 group added to inhibit template jumping. A black hexagon represents the Cy3 group. B, top, SYBR-gold stained denaturing urea-PAGE gel of cDNA products of the BoMoC variants. Far right lane has +0, +1, +2 markers for addition of the corresponding number of nt by NTA. Bottom, quantification of +0 and NTA cDNA products normalized to WT. cDNA, complementary DNA; NTA, nontemplated nucleotide addition.

contact unpaired template (Figs. 3C and S2A), on the opposite side of the active site cleft from the thumb domain (Fig. 3A).

Bypass of an NTA requirement for template jumping

The template-jumping activity of RTs is useful for laboratory applications such as cDNA library synthesis (3, 29). However, it can also complicate cDNA library production by producing nonnative, chimeric cDNAs (37). Therefore, we sought to understand why most low-NTA BoMoC variants (BoMoC R463A, R473A, D500A, F534G, L704A, and F708A) did not generate template-jumping products (Fig. 2B). BoMoC K452A is the exception: it has reduced NTA but still supports template jumping. To this end, we tested template jumping from blunt duplexes or duplexes with primer-strand 3' overhangs. We assayed +1, +2, and +3 nt 3' overhangs representative of different lengths of NTA (Fig. 6A; oligonucleotide

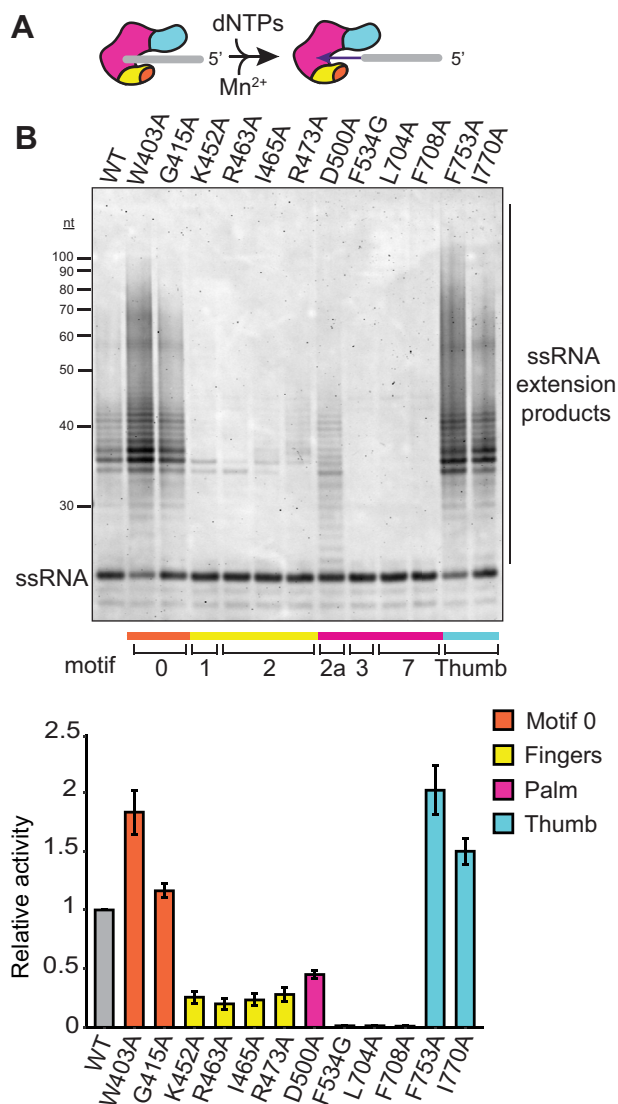








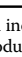
Figure 5. Tailing activity of BoMoC variants. A, diagram depicting BoMoC extension of a ssRNA 3' end in the presence of manganese (Mn^{2+}). B, top, SYBR-gold stained denaturing urea-PAGE gel of ssRNA extension products. Bottom, quantification of ssRNA extension products normalized to WT.

sequences are listed in Table 1). A no enzyme control and no template control were compared to visualize products from NTA without template jumping (Fig. 6B, compare lanes 1–4 and 5–8 in the region labeled primer \pm NTA). The no template control reaction with WT BoMoC and blunt primer duplex had a low level of spurious product formation, which was reduced when reactions also contained a template RNA oligonucleotide (Fig. 6B, compare lanes 5 and 9).

Under assay conditions that are optimal for template jumping, in reactions containing an added oligonucleotide template, WT BoMoC generated detectable cDNA synthesis products with all four primer duplexes, but maximal template jumping occurred with +1 or at most +2 nt of 3' overhang complementary to the template 3' end (Fig. 6B, lanes 9–12, products labeled Template Jumps). With WT BoMoC, NTA to the input primer-template duplex was maximal on the blunt-end substrate (Fig. 6B, lanes 5 and 9; note the products

Non-LTR retroelement reverse transcriptase activities

Table 2
Summary of results

Enzyme		Fill-in cDNA synthesis	NTA profile	Tailing	Jumping after cDNA synthesis	Jump from +2/+1 primer duplex	
Motif	0 	WT	3–4	++	+	1	
		W403A	↑	3–4	++	+	n.d.
		G415A	↑	3–4	++	+	n.d.
Fingers	1 	K452A	↓	0–3	+	~1	
		R463A	↓	0–2	+	>3	
		I465A	↓	2–3	+	–	~1
		R473A	↓	3	+	–	~3
Palm	2 	2a 	D500A	↑	0–3	+	>3
		3 	F534G	↓	0	–	>3
		7 	L704A	↑	0–3	–	~3
		F708A	↑	0–3	–	–	n.d.
Thumb		F753A	↑	3–4	++	+	n.d.
		I770A	↑	3–4	++	+	n.d.

Up-arrows indicate an increase in activity in fill-in cDNA synthesis assays compared to WT and down-arrows indicate a decrease in activity. NTA profile range is given as the most predominant NTA products evident in Figure 2B. Tailing activity is categorized into three levels: two plus signs indicate WT or stronger signal, one plus sign indicates weak activity, and a minus sign indicates no activity. Template jumping after initial primed cDNA synthesis is similarly demarcated by plus and minus signs. “Jump from +2/+1 primer duplex” gives the ratio of template-jumping product synthesis using primer duplexes with +2 or +1 nt overhang, with representative data shown in Figure 6. Enzymes that were not tested or results that were not reliably quantified because of low signal are marked n.d. for not determined. Results in the “Jump from +2/+1 primer duplex” column for BoMoC K452A and I465A are not shown but were performed parallel to assays shown in Figure 6; the primer preference for template jumping by BoMoC K452A and I465A was similar to that of WT BoMoC.

Discussion

Structure/function relationship for a non-LTR RT

B. mori R2 protein is a favorable system for characterization of the biochemical activities of a non-LTR retroelement RT. Previous mutagenesis studies using the full-length R2 protein explored the sequence requirements for nucleic acid binding and EN activity, targeting regions of the protein N- and C-terminal to the core RT domain (46–49). The BoMoC variants described in this work specifically tease apart RT active-site structural requirements for cDNA synthesis, NTA, and template jumping (Table 2), enabling future studies of how these RT activities support non-LTR retroelement mobility. In addition, our results provide a basis for comparison of the active-site architecture of a non-LTR RT and the active sites of retroviral and intron RTs and viral RdRPs. Our findings indicate that protein side chains of the nucleotide-binding pocket and side chains involved in unpaired-template interaction immediately adjacent to the primer duplex have critical contributions to both cDNA synthesis activity and NTA, whereas in contrast motif 0 and thumb-domain side chains do not. The particular motif 0 and thumb-domain substitutions examined in this work actually improve *in vitro* enzyme function in cDNA synthesis and as a terminal transferase in manganese-dependent ssRNA tailing.

The mechanism by which BoMoC thumb-domain F753A and I770A substitutions increase cDNA synthesis activity is likely to involve reduced stability of enzyme interaction with the product-duplex minor groove. A thermostable group II intron RT has thumb domain Y325 (15) in similar position to BoMoC F753. Having a bulky hydrophobic side chain monitoring minor groove geometry serves as a fidelity check and increases affinity for product DNA (45). Thumb-domain

contact with the minor groove contributes to the particularly high processivity of the EuRe group II intron RT (14). Likewise, R2 RT thumb-domain side chains F753 and I770 could be important for the high processivity essential to full-length copying of non-LTR retroelement template RNAs, but assays used in this work do not demand high processivity. When performing cDNA synthesis on relatively short RNA templates, reduced interaction of BoMoC with product duplex could favorably increase the rate of enzyme release and thus allow more cDNA synthesis overall.

In previous work, motif 0 substitutions in full-length *B. mori* R2 RT or a group II intron RT decreased enzyme activity and inhibited template jumping (15, 47). Those studies targeted residues in a conserved P-G-hydrophobic-D-G motif (Fig. S2A, BoMoC sequence PGPDG). When we made BoMoC single amino acid substitutions of each of the previously targeted residues, we observed a similar phenotype (data not shown). The BoMoC motif 0 substitutions assayed in this work were instead made at the base of what is known as Motif G or the “G Loop” of RdRPs (50) or the “RT 0 lid” of a group II intron RT that contains the conserved P-G-hydrophobic-D-G sequence (15). Here, the motif 0 substitutions, W403A and G415A, surprisingly increased BoMoC cDNA synthesis and tailing activities without an apparent change in NTA. Of particular note, removal of the large hydrophobic side chain of W403 did not inhibit template jumping. We suggest that our motif 0 substitutions may have directly or indirectly, through changes in positioning of other motif 0 amino acids, reduced constraints on unpaired template entry into the active site. The WT sequence of motif 0 could be more important for BoMoC cDNA synthesis on its highly structured cellular template than on the oligonucleotide templates used in this work. We are developing cellular assays of RT-mediated gene insertion that

will enable future testing of the consequences of the BoMoC motif 0 side-chain substitutions on retroelement mobility.

Template-jumping requirements of a non-LTR RT

Template jumping is a shared property of retroviral, group II intron, and non-LTR retroelement RTs assayed *in vitro* (3). What governs the ability of a polymerase to support template jumping has been challenging to conclude, largely because of uncertainties in interpreting the comparison of results obtained in different laboratories with different enzymes, templates, and reaction conditions. For example, full-length *B. mori* R2 RT was not thought to support template jumping from a duplexed primer (22), whereas BoMoC does (29). This disparity is more likely to reflect differences in purification and assay conditions than in inherent enzyme properties.

Against our initial expectation, some BoMoC variants compromised for template jumping could be rescued for this activity using a primer duplex with a 2 nt 3' overhang. This finding bolsters a conclusion that template jumping requires prior NTA to a cDNA or primer 3' end (Fig. 6D). We also conclude that dNTP-binding pocket integrity is not critical for template jumping, if the NTA requirement is bypassed by primer design. However, even with bypass of the NTA requirement, BoMoC L704A and F708A variants remained severely compromised for template jumping. Relatively weak rescue of template jumping for these enzymes correlates with their sharply decreased ssRNA tailing activity. How template jumping and tailing are dependent on side chains within the primer grip motif (Fig. S2B), and other side chains near the primer 3' end, will be interesting to investigate in more detail. Independent of the mechanism, the use of BoMoC L704A and F708A enzymes with robust cDNA synthesis activity but severely inhibited template jumping can enable new RT laboratory applications.

For *B. mori* R2 RT and BoMoC, the probability that a 3' overhang created by NTA matches an incoming template 3' end strongly depends on reaction conditions (23, 29). In reactions with balanced concentration of the four dNTPs, the RT adds predominantly non-templated adenosines to generate an at least 3 nt NTA overhang, which is nonproductive for template jumping (29). We suggest that for non-LTR retroelement RTs, as for group II intron and retroviral RTs, template jumping may not be physiologically necessary for retroelement/retrovirus proliferation. Indeed, the inserted cDNA chimeras characterized in human LINE-1 mobility assays arise from preligation of the retroelement transcript to a noncoding RNA, rather than copying of discontinuous templates (51). In future studies, it will be of interest to dissect the biological requirements for template jumping in retroelement mobility using the structure/function insights from this work.

Experimental procedures

Construction of expression vectors and protein purification

The 2Bc-T vector encoding N-terminal maltose-binding protein and C-terminal six-histidine tagged BoMoC (29) was used as a template for site-directed mutagenesis. Intended

changes were confirmed by DNA sequencing. Plasmids were transformed into BL21(DE3) cells and plated, then a single colony was grown in 2xYT media and induced at A₆₀₀ 0.6 to 0.8 at 16 °C overnight with 1 mM Isopropyl β-d-1-thiogalactopyranoside. Cells were harvested by centrifugation at 4000 rpm and lysed in 20 mM Tris pH 7.5, 1 M NaCl, 1 mM MgCl₂, 0.2% NP-40, 10% glycerol, 1 mM DTT, and protease inhibitors. Two-step purification was initiated by allowing lysate protein to bind Nickel-NTA resin for 2 h at 4 °C. After binding, resin was washed three times with 20 mM Tris pH 7.5, 1 M KCl, 20 mM imidazole, 10% glycerol, 0.1% NP-40, and 1 mM DTT. Proteins were subsequently eluted in 20 mM Tris pH 7.5, 0.8 M KCl, 10% glycerol, 1 mM DTT, and 500 mM imidazole. Eluted protein was size-fractionated on a HiLoad 16/600 Superdex 200 pg column in the Nickel-NTA elution buffer without imidazole. Pooled fractions were concentrated using Amicon centrifugal filter units, and protein concentration was quantified by bicinchoninic acid assay. BoMoC protein integrity and purity were validated by Coomassie blue staining after sodium dodecyl sulfate - polyacrylamide gel electrophoresis. Enzyme aliquots were stored at -80 °C. Enzyme working stocks were diluted to 10 μM protein in 25 mM Tris pH 7.5, 200 mM KCl, 400 mM (NH₄)₂SO₄, 50% glycerol, and 2 mM DTT, and stored at -20 °C. Bacterial RT proteins were purified as previously described (29).

Protein structure prediction

The Phyre2 Protein Fold Recognition server was used for protein structure prediction (52). Motifs -1 through the thumb were submitted, of which 85% (435 residues) were modeled at >90% accuracy across two templates described in Results. Intensive mode with default parameters was used. Residues modeled *ab initio* were omitted from the 3D model represented in this work (see Fig. 1 legend). Figure panels containing structure predictions were made using ChimeraX (53).

Activity assays

For cDNA synthesis and NTA assays, 20 μl reactions with 0.5 μM RT protein were carried out in RT buffer (20 mM Tris pH 7.5, 150 mM KCl, 5 mM MgCl₂, 1 mM DTT, 2% PEG-6000, and 500 μM dNTPs), and 200 nM primer duplex. Reactions proceeded for 10 min at 37 °C, followed by heat inactivation at 65 °C for 5 min, then addition of 0.5 μg/μl final concentration of RNase A (Sigma, R6513) with incubation for 15 min at 50 °C. The reactions were stopped with 50 mM Tris pH 7.5, 20 mM EDTA, and 2% SDS. Products were extracted with phenol: chloroform: isoamyl alcohol (25:24:1), isopropanol precipitated using 10 μg glycogen as carrier, and air-dried for 5 min before resuspension in 5 μl 2x formamide loading dye (95% deionized formamide, 0.025% bromophenol blue (w/v), 0.025% xylene cyanol (w/v), and 5 mM EDTA). Products were separated on 15% denaturing urea-PAGE gels then stained using SYBR Gold and imaged by Typhoon Trio.

For terminal transferase tailing assays, the reactions proceeded as above except 5 mM MgCl₂ and 200 nM

Non-LTR retroelement reverse transcriptase activities

primer-duplex were substituted with 5 mM MnCl₂ and 200 nM ssRNA. Products were processed for denaturing PAGE as described above but without the RNase step.

For assays testing rescue of template jumping, nucleotide concentrations were adjusted to 200 μM dTTP, 40 μM dCTP, 40 μM dGTP, and 20 μM dATP. Universal primer duplexes were added at 50 nM, and 3'A jump-acceptor template was added at 200 nM. The reactions were carried out at 37 °C for 10 min, followed by analysis as described above.

Quantification and statistical analyses

All gel quantification was done with ImageJ. All graphical data represents mean ± standard error of three technical replicates wherein three separate reactions were performed and reaction products analyzed on different gels.

Data availability

All data are contained within the article.

Supporting information—This article contains supporting information (54).

Acknowledgments—We thank Collins lab members for discussion and feedback on this work.

Author contributions—S. C. P., H. E. U., and K. C. conceptualization; S. C. P. and H. E. U. methodology; S. C. P. formal analysis; S. C. P. investigation; S. C. P. writing—original draft; S. C. P., H. E. U., and K. C. writing—review and editing; K. C. supervision; K. C. funding acquisition.

Funding and additional information—This work was supported by funding from University of California, Berkeley (Bakar Fellows Program) and the National Institutes of Health (DP1HL156819) to K. C. The content is solely the responsibility of the authors and does not necessarily represent the official views of the National Institutes of Health.

Conflict of interest—BoMoC variants with improved properties are included in patent applications filed by University of California, Berkeley, with S. C. P., H. E. U. and K. C. as named inventors. H. E. U. and K. C. are the founders of Karnateq Inc., which licensed the RT technology.

Abbreviations—The abbreviations used are: cDNA, complementary DNA; EN, endonuclease; LINE, long interspersed nuclear element; LTR, long terminal repeat; NTA, nontemplated nucleotide addition; RdRP, RNA-dependent RNA polymerase; RT, reverse transcriptase; TPRT, target-primed reverse transcription.

References

1. Arkhipova, I. R. (2017) Using bioinformatic and phylogenetic approaches to classify transposable elements and understand their complex evolutionary histories. *Mob. DNA* **6**, 19
2. Gao, L., Altae-Tran, H., Böhning, F., Makarova, K., Segel, M., Schmid-Burgk, J., Koob, J., Wolf, Y., Koonin, E., and Zhang, F. (2020) Diverse enzymatic activities mediate antiviral immunity in prokaryotes. *Science* **369**, 1077–1084
3. Martín-Alonso, S., Frutos-Beltrán, E., and Menéndez-Arias, L. (2021) Reverse transcription: From transcriptomics to genome editing. *Trends Biotechnol.* **39**, 194–210
4. Fujiwara, H. (2015) Site-specific non-LTR retrotransposons. *Microbiol. Spectr.* **3**, 1–16
5. Kazazian, H. H. J., and Moran, J. V. (2017) Mobile DNA in health and disease. *N. Engl. J. Med.* **377**, 361–370
6. Sousa, R. (1996) Structural and mechanistic relationships between nucleic acid polymerases. *Trends Biochem. Sci.* **21**, 186–190
7. Ng, K. S., Arnold, J. J., and Cameron, C. E. (2008) Structure function relationships among RNA dependent RNA polymerases. *Curr. Top. Microbiol. Immunol.* **320**, 137–156
8. Xiong, Y., and Eickbush, T. H. (1988) Similarity of reverse transcriptase-like sequences of viruses, transposable elements, and mitochondrial introns. *Mol. Biol. Evol.* **5**, 675–690
9. Xiong, Y., and Eickbush, T. H. (1990) Origin and evolution of retroelements based upon their reverse-transcriptase sequences. *EMBO J.* **9**, 3353–3362
10. Malik, H. S., Burke, W. D., and Eickbush, T. H. (1999) The age and evolution of non-LTR retrotransposable elements. *Mol. Biol. Evol.* **16**, 793–805
11. Blocker, F. J., Mohr, G., Conlan, L. H., Qi, L., Belfort, M., and Lambowitz, A. M. (2005) Domain structure and three-dimensional model of a group II intron encoded reverse transcriptase. *RNA* **11**, 14–28
12. Mahbub, M. M., Chowdhury, S. M., and Christensen, S. M. (2017) Globular domain structure and function of restriction-like-endonuclease LINEs: Similarities to eukaryotic splicing factor Prp8. *Mob. DNA* **8**, 16
13. Mitchell, M., Gillis, A., Futahashi, M., Fujiwara, H., and Skordalakes, E. (2010) Structural basis for telomerase catalytic subunit TERT binding to RNA template and telomeric DNA. *Nat. Struct. Mol. Biol.* **17**, 513–518
14. Zhao, C., and Pyle, A. M. (2016) Crystal structures of a group II intron maturase reveal a missing link in spliceosome evolution. *Nat. Struct. Mol. Biol.* **23**, 558–565
15. Stamos, J. L., Lentzsch, A. M., and Lambowitz, A. M. (2017) Structure of a thermostable group II intron reverse transcriptase with template-primer and its functional and evolutionary implications. *Mol. Cell* **68**, 926–939
16. Ghanim, G. E., Fountain, A. J., van Roon, A. M., Rangan, R., Das, R., Collins, K., and Nguyen, T. H. D. (2021) Structure of human telomerase holoenzyme with bound telomeric DNA. *Nature* **593**, 449–453
17. He, Y., Wang, Y., Liu, B., Helmling, C., Sušac, L., Cheng, R., Zhou, Z., and Feigon, J. (2021) Structures of telomerase at several steps of telomere repeat synthesis. *Nature* **593**, 454–459
18. Craig, R., Yushenova, I., Rodriguez, F., and Arkhipova, I. (2021) An ancient clade of Penelope-like retroelements with permuted domains is present in the green lineage and protists, and dominates many invertebrate genomes. *Mol. Biol. Evol.* **28**, msab225
19. Eickbush, T. H., and Eickbush, D. G. (2015) Integration, regulation, and long-term stability of R2 retrotransposons. *Microbiol. Spectr.* **3**, MDNA3-0011-2014
20. Luan, D. D., Korman, M. H., Jakubczak, J. L., and Eickbush, T. H. (1993) Reverse transcription of R2Bm RNA is primed by a nick at the chromosomal target site - a mechanism for non-LTR retrotransposition. *Cell* **72**, 595–605
21. Cost, G. J., Feng, Q., Jacquier, A., and Boeke, J. D. (2002) Human L1 element target-primed reverse transcription *in vitro*. *EMBO J.* **21**, 5899–5910
22. Bibillo, A., and Eickbush, T. H. (2002) The reverse transcriptase of the R2 non-LTR retrotransposon: Continuous synthesis of cDNA on non-continuous RNA templates. *J. Mol. Biol.* **316**, 459–473
23. Bibillo, A., and Eickbush, T. H. (2004) End-to-end template jumping by the reverse transcriptase encoded by the R2 retrotransposon. *J. Biol. Chem.* **279**, 14945–14953
24. Menéndez-Arias, L., Sebastián-Martín, A., and Álvarez, M. (2017) Viral reverse transcriptases. *Virus Res.* **234**, 153–176
25. Kim, M. J., and Kao, C. (2001) Factors regulating template switch *in vitro* by viral RNA dependent RNA polymerases: Implications for RNA-RNA recombination. *Proc. Natl. Acad. Sci. U. S. A.* **98**, 4972–4977

26. Zhu, Y. Y., Machleder, E. M., Chenchik, A., Li, R., and Siebert, P. D. (2001) Reverse transcriptase template switching: A SMART approach for full-length cDNA library construction. *Biotechniques* **30**, 892–897
27. Oz-Gleenberg, I., and Hizi, A. (2011) Strand selections resulting from the combined template-independent DNA synthesis and clamp activities of HIV-1 reverse transcriptase. *Biochem. Biophys. Res. Commun.* **408**, 482–488
28. Mohr, S., Ghanem, E., Smith, W., Sheeter, D., Qin, Y., King, O., Polio-udakis, D., Iyer, V. R., Hunnicke-Smith, S., Swamy, S., Kuersten, S., and Lambowitz, A. M. (2013) Thermostable group II intron reverse transcriptase fusion proteins and their use in cDNA synthesis and next-generation RNA sequencing. *RNA* **19**, 958–970
29. Upton, H. E., Ferguson, L., Temoche-Diaz, M. M., Liu, X.-M., Pimentel, S. C., Ingolia, N. T., Schekman, R., and Collins, K. (2021) Low-bias ncRNA libraries using ordered two-template relay: Serial template jumping by a modified retroelement reverse transcriptase. *Proc. Natl. Acad. Sci. U. S. A.* **118**, e2107900118
30. Chen, D., and Patton, J. T. (2001) Reverse transcriptase adds non-templated nucleotides to cDNAs during 5'-RACE and primer extension. *Biotechniques* **30**, 574–580
31. Golinelli, M. P., and Hughes, S. H. (2002) Nontemplated nucleotide addition by HIV-1 reverse transcriptase. *Biochemistry* **41**, 5894–5906
32. Golinelli, M. P., and Hughes, S. H. (2002) Nontemplated base addition by HIV-1 RT can induce nonspecific strand transfer *in vitro*. *Virology* **294**, 122–134
33. Oz-Gleenberg, I., Herzig, E., and Hizi, A. (2012) Template-independent DNA synthesis activity associated with the reverse transcriptase of the long terminal repeat transposon Tf1. *FEBS J.* **279**, 142–153
34. Zajac, P., Islam, S., Hochgerner, H., Lönnerberg, P., and Linnarsson, S. (2013) Base preferences in non-templated nucleotide incorporation by MMLV-derived reverse transcriptases. *PLoS One* **8**, e85270
35. Ohtsubo, Y., Nagata, Y., and Tsuda, M. (2017) Efficient N-tailing of blunt DNA ends by Moloney murine leukemia virus reverse transcriptase. *Sci. Rep.* **7**, 41769
36. Wulf, M. G., Maguire, S., Humbert, P., Dai, N., Bei, Y., Nichols, N. M., Corrêa, I. R. J., and Guan, S. (2019) Non-templated addition and template switching by Moloney murine leukemia virus (MMLV)-based reverse transcriptases co-occur and compete with each other. *J. Biol. Chem.* **294**, 18220–18231
37. Lentzsch, A. M., Yao, J., Russell, R., and Lambowitz, A. M. (2019) Template-switching mechanism of a group II intron-encoded reverse transcriptase and its implications for biological function and RNA-Seq. *J. Biol. Chem.* **294**, 19764–19784
38. Lentzsch, A., Stamos, J., Yao, J., Russell, R., and Lambowitz, A. (2021) Structural basis for template switching by a group II intron-encoded non-LTR-retroelement reverse transcriptase. *J. Biol. Chem.* **297**, 100971
39. Galej, W. P., Oubridge, C., Newman, A. J., and Nagai, K. (2013) Crystal structure of Prp8 reveals active site cavity of the spliceosome. *Nature* **493**, 638–643
40. Basu, A., Basu, S., and Modak, M. J. (1989) Site-directed mutagenesis of Moloney murine leukemia virus reverse transcriptase. Demonstration of lysine 103 in the nucleotide binding site. *J. Biol. Chem.* **265**, 17162–17166
41. Sarafianos, S. G., Pandey, V. N., Kaushik, N., and Modak, M. J. (1995) Site directed mutagenesis of arginine 72 of HIV-1 reverse transcriptase. Catalytic role and inhibitor sensitivity. *J. Biol. Chem.* **270**, 19729–19735
42. Chowdhury, K., Kaushik, N., Pandey, V. N., and Modak, J. M. (1996) Elucidation of the role of Arg 110 murine leukemia virus reverse transcriptase in the catalytic mechanism: Biochemical characterization of its mutant enzymes. *Biochemistry* **35**, 16610–16620
43. Gao, G., Orlova, M., Georgiadis, M. M., Hendrickson, W. A., and Goff, S. P. (1997) Conferring RNA polymerase activity to a DNA polymerase: A single residue in reverse transcriptase controls substrate selection. *Proc. Natl. Acad. Sci. U. S. A.* **94**, 407–411
44. Gholamalipour, Y., Karunanayake Mudiyansele, A., and Martin, C. T. (2018) 3' end additions by T7 RNA polymerase are RNA self-templated, distributive and diverse in character-RNA-Seq analyses. *Nucl. Acids Res.* **46**, 9253–9263
45. Menéndez-Arias, L. (2002) Molecular basis of fidelity of DNA synthesis and nucleotide specificity of retroviral reverse transcriptases. *Prog. Nucleic Acid Res. Mol. Biol.* **71**, 91–147
46. Yang, J., Malik, H. S., and Eickbush, T. H. (1999) Identification of the endonuclease domain encoded by R2 and other site-specific, non-long terminal repeat retrotransposable elements. *Proc. Natl. Acad. Sci. U. S. A.* **96**, 7847–7852
47. Jamburuthugoda, V. K., and Eickbush, T. H. (2014) Identification of RNA binding motifs in the R2 retrotransposon-encoded reverse transcriptase. *Nucl. Acids Res.* **42**, 8405–8415
48. Govindaraju, A., Cortez, J. D., Reveal, B., and Christensen, S. M. (2016) Endonuclease domain of non-LTR retrotransposons: Loss-of-function mutants and modeling of the R2Bm endonuclease. *Nucl. Acids Res.* **44**, 3276–3287
49. Pradhan, M., Govindaraju, A., Jagdish, A., and Christensen, S. M. (2020) The linker region of LINES modulates DNA cleavage and DNA polymerization. *Anal. Biochem.* **603**, 113809
50. Wang, M., Li, R., Shu, B., Jing, X., Ye, H.-Q., and Gong, P. (2020) Stringent control of the RNA-dependent RNA polymerase translocation revealed by multiple intermediate structures. *Nat. Commun.* **11**, 2605
51. Moldovan, J. B., Wang, Y., Shuman, S., Mills, R. E., and JV, M. (2019) RNA ligation precedes the retrotransposition of U6/LINE-1 chimeric RNA. *Proc. Natl. Acad. Sci. U. S. A.* **116**, 20612–20622
52. Kelley, L. A., Mezulis, S., Yates, C. M., Wass, M. N., and Sternberg, M. J. (2015) The Phyre2 web portal for protein modeling, prediction and analysis. *Nat. Protoc.* **10**, 845–858
53. Pettersen, E. F., Goddard, T. D., Huang, C. C., Meng, E. C., Couch, G. S., Croll, T. I., Morris, J. H., and Ferrin, T. E. (2021) UCSF ChimeraX: Structure visualization for researchers, educators, and developers. *Protein Sci.* **30**, 70–82
54. Berezin, C., Glaser, F., Rosenberg, J., Paz, I., Pupko, T., Fariselli, P., Casadio, R., and Ben-Tal, N. (2004) ConSeq, The identification of functionally and structurally important residues in protein sequences. *Bioinformatics* **20**, 1322–1324